

# CHARACTERIZATION OF THE LOWER LIMB SOFT TISSUES IN PEDESTRIAN FINITE ELEMENT MODELS

**Costin Untaroiu**

**Kurosh Darvish**

**Jeff Crandall**

Center of Applied Biomechanics, University of Virginia

**Bing Deng**

**Jenne-Tai Wang**

General Motors Research & Development, Warren, MI  
United States

Paper Number 05-0250

## ABSTRACT

Current finite element (FE) models of the human lower extremity lack accurate material properties of the soft tissues (flesh, fat, and knee ligaments), which are needed for computational evaluation of pedestrian injuries. Medial collateral ligament (MCL) is the most frequently injured ligament in lateral impacts. Therefore, the accuracy of the viscoelastic mechanical properties of the MCL FE model is of crucial importance in modeling pedestrian impacts. During automotive impacts, the flesh and fat get compressed, absorb part of the impact energy, and transfer and distribute the rest of energy to the skeleton. Therefore, the compressive response of these soft tissues can affect the accuracy of bone fracture predictions and as a result the overall kinematics of the FE pedestrian model. Quasi-Linear Viscoelastic (QLV) constitutive material models were assumed for MCL, flesh, and fat. Their global properties in terms of material parameters were derived using uni-axial step and hold tests on cadaveric specimens. The material models coefficients were derived by optimization. The flesh/fat models were validated in lateral leg impact tests at 2.5 m/s. The force-deflection results of the impactor, compared to other models, showed more biofidelity with respect to the cadaveric and volunteer data.

## INTRODUCTION

In the past decade, several finite element (FE) lower limb models have been developed in order to reproduce lower limb injuries in the car-to-pedestrian collisions (CPC). Initially (e.g. Bermond et al. [1]) the surrounding muscles and the skin were neglected, and the knee ligaments were modeled usually by spring elements. Recently, due to rapid and continuously increasing of the speed of

computers, more sophisticated FE lower limb models have been developed. These models have accurate geometry obtained from CT and MRI scans from human volunteers (Beillas et al. [2], Takahashi et al [3]) or from Visible Human Database (Untaroiu et al. [4]), and the flesh and knee ligaments were meshed with shell and solid elements. However, the accuracy of FE models depends not only on the quality of the model geometry (e.g. anatomical surfaces, the number of components modeled, or mesh quality), but also on the biofidelity of the material properties assigned to the FE components.

Flesh and skin (fat) cover long bones of the lower limb. During automotive impacts, these soft tissues get compressed, absorb part of the impact energy, and transfer and distribute the rest of energy to the skeleton. Therefore, the compressive response of these soft tissues affect the severity of bone injuries and as a result the overall kinematics of the FE pedestrian/occupant model. McElhaney [5] conducted in-vitro compression tests of bovine muscle along the direction of the fibers. He published the loading stress-strain curves at various strain rates, but the strain data was limited to strains above 35%. The loading in a pedestrian impact is typically transverse to the muscle fiber direction. Therefore, the material properties derived in [5] may not be applicable. However, due to the lack of additional test data, in human FE models reported in the literature (e.g. [2]), it was assumed that the muscle and fat were linear elastic with Young's modulus about 1 MPa based McElhaney's stress-strain curves. In lower extremities of the H-Model [6] the flesh properties were estimated using impact tests on anterior and posterior thigh and the greater trochanter of human volunteers. The flesh material properties were expressed in the form of a nonlinear viscoelastic model that consisted of a nonlinear elastic stiffness in parallel with a viscous damper.

The nonlinearity of spring and damper depended on the ratio of the current to the initial volume. Considering the fact that soft tissues are almost incompressible (volume ratio is almost one) and highly viscoelastic, this material model could simplify their behavior. Snedeker et al. [7] and Ruan et al. [8] used the linear viscoelastic materials for flesh FE models and elastic material for skin models, but significant differences (more ten times) appear between their parameters. All these facts suggest the need for further investigation of the material properties of lower limb flesh and skin.

Medial collateral ligament (MCL) is the most frequently injured ligament in lateral impacts. Therefore, the accuracy of the viscoelastic mechanical properties of the MCL FE model is of crucial importance in modeling pedestrian impacts. MCL, as all knee ligaments, is highly anisotropic material consisting of a ground substance material reinforced by collagen and elastin (Weiss and Gardiner [9]). Collagen provides the major resistance in tension and negligible resistance in compression. In the literature, the mechanical properties of ligaments are provided as structural properties (derived from tensile test of the bone-ligament-bone structures), or material properties (derived from tests on isolated ligaments tissues). Structural properties depend on the global material properties, the direction in which the ligament is pulled, and the rate of loading. In FE models, the structural properties can be used only if the ligaments are modeled with one-dimensional elements (linear or non-linear springs). However, this approach is incapable of simulating the bone-ligament and ligament-ligament contacts, cross-sectional variation of ligament, and the stress distribution around the insertion sites. For two-dimensional (shell) or three-dimensional (solid) representations of ligaments, the material constitutive properties are needed. However, in the literature only one study reported material property data of MCL. Quapp and Weiss [10] conducted tensile tests at a strain rate of 1% sec<sup>-1</sup> on dog-bone shaped samples taken from the anterior-central two-third regions of ten human MCLs along the collagen fiber direction (longitudinal). The material properties obtained along the collagen axis were close to the average data reported by Butler et al. [11] (average of LCL, PCL, and ACL), and it was twenty times stiffer than the properties found in the transverse direction. Anisotropic hyper-elastic constitutive models were used to describe the tensile properties in both directions. The material coefficients were obtained by optimization. MCL is also a viscoelastic material, but its viscoelasticity in the domain of milliseconds, characteristic to the car crashes, is poorly understood. Woo et al [12] determined the material properties of

rabbit MCLs at five strain rates, from 0.008 mm/sec to 113 mm/sec. Tensile strength and ultimate strain increased slightly with increasing strain rate, whereas tangent modulus remained essentially unchanged. Based on this Weiss and Gardiner [9] concluded that the strain rate dependency had relatively small effects on ligament material properties. Yamamoto et al. [13] conducted dynamic tensile tests with femur-MCL-tibia complex obtained from female Japanese white rabbits. The strain rate was changed from 0.01 mm/sec to 300 mm/sec and a significant strain rate dependency was observed for the entire region of the stress-strain curve. The brief review of the reported material properties for MCL shows that its material properties, especially the viscoelastic ones, are poorly understood and need for further investigation.

The objectives of this work were to determine the material properties of lower limb soft tissues (flesh, fat, and MCL) and to evaluate their ability to describe the global response of the corresponding human tissues. To achieve these objectives, step and hold uniaxial tests on cadaveric specimens were performed. According to the main loadings which appear in the soft tissues during the pedestrian accidents, the flesh and fat samples were loaded in compression, while bone-MCL-bone complex was loaded in tension. The quasi-linear viscoelastic theory (QLV) [14] was selected to characterize the properties of the soft tissues under study. The material model coefficients were derived by optimization.

## MATERIAL IDENTIFICATION

### Quasi-Linear Viscoelastic (QLV) Theory

Soft tissues have a time-dependent behavior which can arise from fluid flow in and out of the tissue, or from inherent viscoelasticity of the solid phase (Weiss and Gardiner [9]). Fung [14] has proposed the QLV theory which had been widely used in mechanics in order to describe the soft tissue behavior. The main assumption of this theory is that the elastic response and the relaxation function are separated in the convolution integral representation of the stress, as shown in the following expression for a uniaxial loading condition:

$$\sigma(t) = \int_0^t G(t-\tau) \frac{\partial \sigma^e[\lambda(\tau)]}{\partial \tau} d\tau \quad (1).$$

where  $\sigma^e$  is the elastic response,  $G(t)$  the relaxation function, and  $\lambda(t)$  is the stretch ratio time history. A material model with this formulation implemented in Ls-Dyna was used in the material identification processes. A brief description of this material model is provided in this section.

The soft tissue is considered as a composite material which consists of collagen fibers embedded in a softer isotropic (ground) material. The strain energy function of the soft tissue material, as was formulated by Weiss [15], has three terms:

$$W = W_1 + W_2 + W_3 \quad (2).$$

The first term models the ground substance matrix as a Mooney-Rivlin material:

$$W_1 = C_1(I_1 - 3) + C_2(I_2 - 3) \quad (3).$$

where  $I_1$  and  $I_2$  are the invariants of the right Cauchy deformation tensor. The second term  $W_2 = F(\lambda)$  is defined to capture the behavior of crimped collagen in tension and it works only in the fiber direction defined in the model. Its derivative (i.e., stress) has an exponential function which describes the straightening of the fibers and a linear function once they are straightened past a critical stretch level  $\lambda^*$ :

$$\frac{\partial F(\lambda)}{\partial \lambda} = \begin{cases} 0 & \lambda < 1 \\ \frac{C_3}{\lambda} [\exp(C_4(\lambda - 1)) - 1] & \lambda < \lambda^* \\ \frac{1}{\lambda} (C_5\lambda + C_6) & \lambda \geq \lambda^* \end{cases} \quad (4).$$

The role of the last term in the strain energy function is to ensure nearly-incompressible material behavior:

$$W_3 = \frac{1}{2} K [\ln(J)]^2 \quad (5).$$

where  $J = \det \mathbf{F}$  is the third invariant of the deformation tensor (change in volume) and  $K$  is the bulk modulus. It is recommended that the bulk modulus should be two-three orders of magnitude larger than  $C_1$ . The reduced relaxation function  $G(t)$  was represented by a Prony series:

$$G(t) = \sum_{i=1}^3 S_i \exp\left(\frac{-t}{T_i}\right) \quad (6).$$

where  $S_i$  and  $T_i$  terms are the spectral strengths and characteristics times. Three terms were used for MCL and two terms for flesh and skin,

### MCL Material Identification

A representative bone-MCL-bone specimen was extracted while its ends were potted in the fully extended position. The proximal potting cup was rigidly fixed and the distal cup was pulled along the longitudinal axis of tibia. First, the specimen was subjected to a ramp-and-hold test with constant tensile ramp of 3 mm in 30 ms and approximately

600 seconds hold time. The second test was a quasi-static test to failure on the same specimen. In both tests the time histories of force and displacement were recorded. For MCL material identification, the components of the UVA-GM FE model [4] were used (Figure 1).

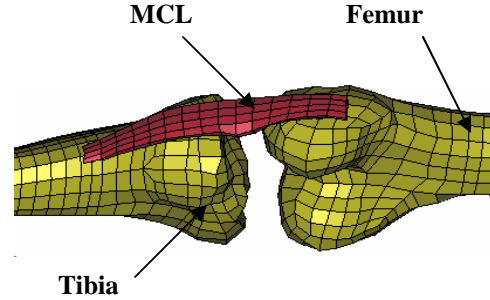


**Figure 1. FE Simulation of the MCL Tensile Tests.**

The MCL specimen had geometrical characteristics (length and medial cross-section) close to the MCL FE model. The insertion sites in the model were created using tied contact between bones and ligament. The direction of anisotropy (of collagen fibers) was defined in the material definition as the element normal in the longitudinal direction as illustrated in Figure 2.

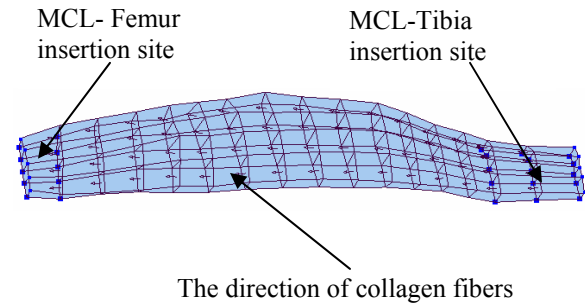


**Figure 2. The insertion sites of MCL FE model and the direction of collagen fibers.**

First, the quasi-static test was simulated. The material coefficients were optimized, assuming the quasi-static test data as the target values and defining minimization of the root-mean-square (RMS) error as the objective function. The optimization process was performed using the response surface methodology (RSM), a statistical method implemented in LS-Opt [16], used usually in design optimization. The hyperelastic coefficients ( $C_1$ - $C_3$ ) were considered as design variables (independent parameters). The design space (a multi-dimensional space) was defined

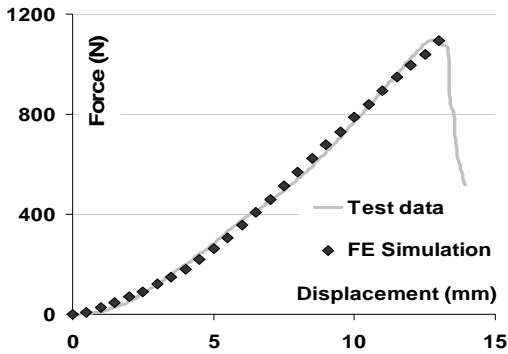


**Figure 3. Quasistatic tensile test of MCL; Comparison between the test data and FE simulation results.**

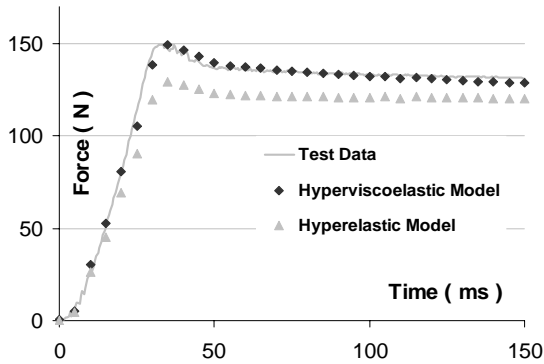


**Figure 4. Dynamic tensile test of MCL; Comparison between test data and FE simulation results.**

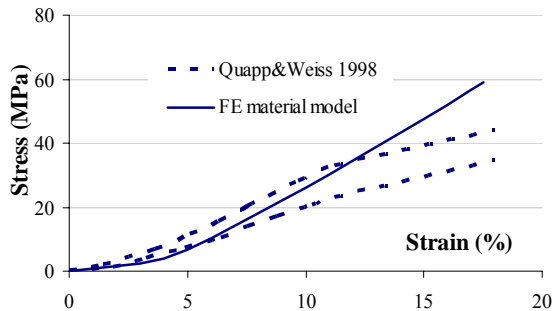


**Figure 5. MCL stress-strain relationship; comparison between the material model determined from FE optimization and data reported by Quapp and Weiss [10].**

as the ranges of hyperelastic coefficients, which were based on the data reported in [10]. The “best” design point (the set of hyperelastic coefficients provided in Table 1) were determined iteratively based on the

**Table 1. Optimized MCL material properties.**

K (GPa)	C <sub>1</sub> (MPa)	C <sub>3</sub> (MPa)	C <sub>4</sub> -	C <sub>5</sub> (MPa)	S <sub>1</sub> -
3.75	7.85	0.25	60.4	307.5	0.15
S <sub>2</sub> -	S <sub>3</sub> -	T <sub>1</sub> (ms)	T <sub>2</sub> (ms)	T <sub>3</sub> (ms)	λ
0.026	0.348	100	11,710	162,633	1.05

responses (RMS errors) at the design points, which were optimally distributed throughout the design space.

The viscoelastic properties of the ligament were then determined from the dynamic ramp and hold test. A three-term Prony series was considered to characterize the MCL relaxation behavior. The long-term Prony coefficients (S<sub>3</sub> and T<sub>3</sub>) were estimated directly from the relaxation data. The two additional Prony coefficients (S<sub>1</sub>, T<sub>1</sub>, S<sub>2</sub>, and T<sub>2</sub>) were determined by considering both the ramp and hold periods and the same FE optimization procedure described above was conducted. All MCL material coefficients obtained by FE optimization are provided in Table 1.

The results of the simulations of quasi-static failure tests and dynamic ramp-and-hold tensile tests of MCL in comparison with experimental data are shown in Figures 3, and 4 respectively. The elastic stress-strain relationship in a cubic sample of MCL in tension along the collagen fibers with optimized parameters was compared with the corridor provided in Quapp and Weiss [10].

### Flesh and Fat Material Identification

The dynamic passive properties of flesh and fat were determined from step and hold unconfined compression tests on cadaveric samples, as shown in Figure 6. Rectangular samples (20mm length and width, and 7 mm thickness) were excised perpendicular to the longitudinal axis of the leg from anterior thigh muscles and fat. Four flesh sample and one fat sample were tested. Approximately 20% compression was applied in 60 ms.

Structurally, fat tissue has no preferred direction and therefore can be considered to be isotropic. Muscle tissue however can be assumed to be transversely isotropic with the axis of anisotropy being along the longitudinal axis of the muscle. Since compression tests were performed perpendicular to this axis, the muscle samples were assumed also to be isotropic. As most of the other soft tissues, both muscle and fat were assumed to be nearly incompressible. The material properties were

assumed to be visco-hyperelastic with a Mooney-Rivlin strain energy function (Equation 3).

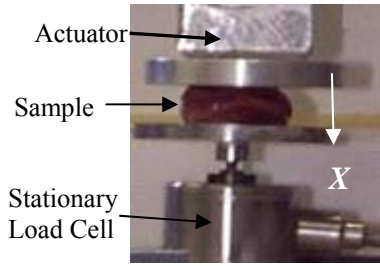


**Figure 6. The apparatus for unconfined compression tests with a muscle sample.**

Based on the boundary conditions on the unloaded faces ( $X_2$  and  $X_3$ ) of the sample and the incompressibility condition, the elastic stress in the compression direction ( $X_1$ ) can be derived as:

$$\sigma_{1m}^e = \frac{2(\lambda_1^3 - 1)}{\lambda_1^2} (C_1 \lambda_1 + C_2) \quad (7).$$

Where  $\lambda_1(t)$  is the stretch ratio history that was derived from the actuator displacement. The experimental Cauchy stress history was calculated based on the compression force history  $F(t)$  measured by the load cell and the initial cross-sectional area  $A_0$  with the following formula:

$$\sigma_{1\text{exp}}^e(t) = \frac{F(t)}{A_0 \lambda_1^2(t)} \quad (8).$$

Assuming a relaxation function of exponential form as shown in (6), the model and experimental Cauchy time histories were derived recursively from the convolution integral (Equation 1). The actual ramp and hold inputs were used as arbitrary inputs and the convolution integral of Equation (1) was carried out numerically as in Puso and Weiss [17]. The material coefficients  $C_i$  and the coefficients of Prony series  $S_i$  and  $T_i$  were optimized, assuming the experimental Cauchy stresses (Equation 8) as the target values and defining minimization of the root-mean-square (RMS) error as the objective function. Minimization was carried out using the Solver package of Microsoft Excel, which uses a quasi-Newton search algorithm. A comparison between the Cauchy stress obtained from experimental data and the stress calculated from the model using the optimized parameters is shown in Figure 7. The average reduced relaxation function of flesh (muscle) and the reduced relaxation function of fat are shown in

Figure 8. The average material properties obtained from flesh tests and fat data are provided in Table 2.

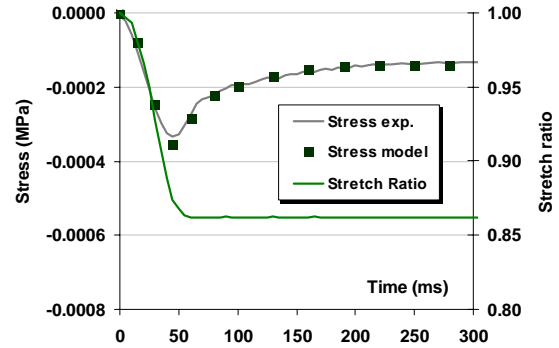


**Figure 7. Comparison between the experimental and model results for flesh.**

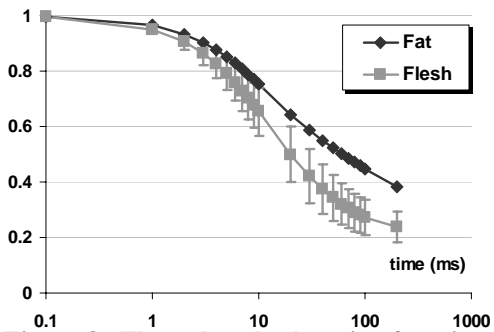


**Figure 8. The reduced relaxation functions of flesh and fat.**

**Table 2. Material Properties of Flesh and Fat.**

Tissue	$C_1$ (kPa)	$C_2$ (kPa)	$S_1$	$S_2$	$T_1$ ms	$T_2$ ms	$K$ MPa
Muscle	0.12	0.25	1.2	0.8	23	63	20
Fat	0.19	0.18	1.0	0.9	10	84	20

## FLESH VALIDATION AT LATERAL IMPACT

In order to verify the global response of the QLV material models of flesh and skin developed in this study, the lateral impact tests to the leg performed by Dhaliwal et al. [18] were simulated. The optimized material properties were assigned to the flesh and skin in the lower limb finite element (FE) model of the 50th percent male developed by Untaroiu et al [4].

The femoral head, distal fibula/tibia, and the skin nodes in contact with rigid foam blocks (on the opposite side of the impact) were rigidly constrained.

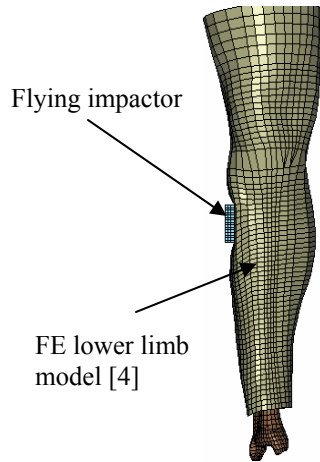


**Figure 9. The impactor hitting the FE model.**

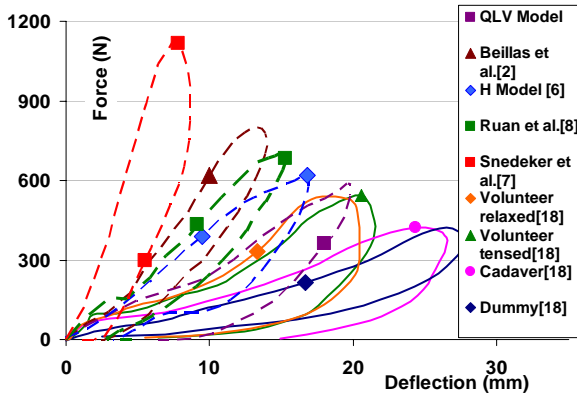


**Figure 10. Force-deflection response; Comparison between FE simulation with QLV skin/flesh material models, other published models, and typical test data [18].**

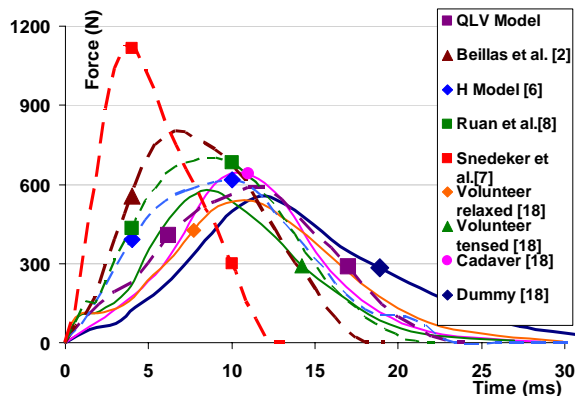


**Figure 11. Impact Force time histories; Comparison between FE simulation with QLV skin/flesh material models, other published models, and typical test data [18].**

The free flying impactor was a plate (45 mm by 142 mm – impact area) with 1.84 kg mass and 2.5 m/s initial velocity, as illustrated in Figure 9. The impact direction was inclined 30 degrees from the lateral direction as in [18] to protect the fibula. The densities of muscle and fat were assigned as 1000, and 800 kg/m<sup>3</sup> respectively. In simulations, the impactor force and displacement of one point of the impactor were calculated. The ratio of the energy lost by the impactor was obtained based on the initial velocity  $V_{initial}$  and the rebounded velocity  $V_{rebound}$ , as in [18]:

$$E = \left[ 1 - \left( \frac{V_{rebound}}{V_{initial}} \right)^2 \right] \cdot 100 \quad (9).$$

Several simulations of the lateral impact test were run with other published flesh/skin material models mentioned before. Their simulation results, the results of the FE model with QLV skin/flesh models, typical test data of cadavers, Hybrid III dummy, and volunteers with relaxed and tensed muscles [18] were compared in terms of force-deflection response and the impact force histories in Figures 10, and 11 respectively. Some characteristic parameters reported in [18] and their range from test data were compared to FE simulation results in the Table 3.

**Table 3. Comparison between test data [18] and FE simulation results for different flesh/skin material models used in the FE lower limb model. (Numbers in paranthesis indicate S.D.)**

Specimen/ FEM - skin/flesh material models	Max. Force (N)	Max. defl. (mm)	Impact Time (ms)	Energy Lost Ratio (%)
<b>Relaxed Volunteer</b>	498 (52)	21 (3)	24 (2)	82 (4)
<b>Tensed Volunteer</b>	521 (62)	20 (4)	24 (1.8)	74 (4)
<b>Cadaver</b>	596 (168)	22 (3)	24.2 (5.6)	82 (2)
<b>Dummy</b>	535 (8)	24 (0.1)	34.2 (0.5)	60 (1)
<b>FEM – [2]</b>	802	14	18	45
<b>FEM – [6]</b>	617	17	24	56
<b>FEM – [7]</b>	1114	8.7	12.2	64
<b>FEM – [8]</b>	702	15.3	21.5	41
<b>QLV material</b>	592	20	24	64

## DISCUSSION

The QLV material model developed in this study for MCL showed good agreement with experimental data in tensile tests. In the dynamic test with 0.1 mm/ms displacement rate, approximately 15% increase in the peak dynamic force was observed, which suggests that tissue viscoelasticity plays an important role in the response during impact scenarios. The elastic stress-strain relationship of the model in tension along the collagen fibers was compared with the corridor provided in Quapp and Weiss [10]. The current material model was slightly stiffer at strains above 13% (Figure 5). This material model was determined by assuming a homogeneous anisotropic material for the whole MCL and optimizing its global tensile properties. However, MCL is inhomogeneous, particularly at the insertion sites, which could explain the difference observed in its local and global properties.

The global responses of the QLV skin/flesh material models developed in this study and other material models from the literature were compared with the published experimental data [18] for cadavers, Hybrid III dummy, and volunteers with relaxed and tensed muscles. The model results using the identified material properties showed good agreement with the cadaver data in terms of the maximum force and displacement. The ratio of energy loss (calculated based on the initial and rebound velocities) was 64%, which was smaller than the volunteer data (70-86%), but larger than the dummy data (60%), or other published material models (41-64%). Such difference could appear due to inaccuracies in the determination of the Pony series coefficients as a result of the optimization procedure, the number of relaxation terms (three), the hold time (500 ms), and the limited number of cadaveric specimens tested. Also friction at the impactor/skin interface contributes to the energy loss whereas in the FE simulation no friction was applied at the contact interface. Overall, the model with QLV material property showed significantly better biofidelity than the model with linear elastic property in low speed impact tests.

The main limitation of the QLV soft tissues material models developed in this study is determined by the small number of samples used in the material identification processes. Since the MCL geometry is not identical in all subjects, it is advisable that an FE model should be developed for each specimen based on its surface digitization. In case of compressive material properties of flesh/skin, more validations are needed especially at high speed impacts.

## CONCLUSIONS

The global viscoelastic material properties of a representative MCL specimen were derived by FE optimization. Results showed a higher stiffness at high strain values than the local properties derived in a previous study. The viscoelastic properties obtained from the stress relaxation tests showed that tissue viscoelasticity increases the peak dynamic force by 15% at 0.1 mm/ms displacement rate. Studies of more specimens are underway and will be reported in the future.

The passive material properties of muscle and fat were identified from unconfined compression tests on cadaveric samples using a QLV constitutive material model. The global validation performed against published lateral impact test data using actual flesh/skin models showed more biofidelity than other material models used in the literature. The high stiffness of several published muscle/skin models poses a question over the accuracy of the global validation results in which the skin was impacted. More validation tests are needed for the wide range of impact speeds observed in car-to-pedestrian collisions.

## REFERENCES

- [1] Bermond, F.; M. Ramet; R. Bouquet and D. Cesari (1994). "A finite element model of the pedestrian leg in lateral impact." 14th ESV.
- [2] Beillas, P.; P.C. Bageman; K.H. Yang; A.I. King; P.J. Arnoux; H.S. Kang; K. Kayvantash; C. Brunet C.; C. Cavallero and P. Prasad P., 2001, "Lower Limb: Advanced FE Model and New Experimental Data." *Stapp Car Crash Journal* 45: 469-494.
- [3] Takahashi, Y.; Y. Kikuki; F. Mori, and A. Konosu (2003). "Advanced FE Lower Limb for Pedestrians.", 18th ESV Conference
- [4] Untaroiu, C., Darvish, K., Crandall, J., Deng, B., and Wang J.T., 2004, "Development and Validation of a Finite Element Model of the Lower Limb", IMECE 2004-61583, 2004 ASME Congress.
- [5] McElhaney, J., 1966, "Dynamic response of bone and muscle tissue," *Journal of Applied Physiology*, 21(4): 1231-1236.
- [6] "H-Dummy™ Version 2.1 User's Manual", (1999). Hankook ESI, Engineering Systems International

[7] Snedeker, J.G., M.H. Muser, and F.H. Walz (2003). "Assessment of Pelvis and Upper Leg Injury Risk in Car-Pedestrian Collisions: Comparison of Accident Statistics, Impactor Tests and a Human Body Finite Element Model", *Stapp Car Crash Journal*, 47:437-457

[8] Ruan, J., R. El-Jawahri, L. Chai, S. Barbat, and P. Prasad (2003). "Prediction and Analysis of Human Thoracic Impact Responses and Injuries in Cadaver Impacts Using a Full Human Body Finite Element Model" *Stapp Car Crash Journal*, 47:299-321

[9] Weiss, J.A. and J.C. Gardiner (2001). "Computational Modeling of Ligament Mechanics." *Critical Reviews in Biomedical Engineering* 29(4): 1-70

[10] Quapp, K.M. and J.A. Weiss (1998). "Material Characterization of Human Medial Collateral Ligament." *Journal of Biomechanical Engineering* 120: 757-763.

[11] Butler, D.L.; M.D. Kay, and D.C. Stouffer (1986). "Comparison of Material Properties in Fascicle-Bone Units from Human Patellar Tendon and Knee Ligaments." *Journal of Biomechanics* 19(6): 425-432.

[12] Woo, S.L.; M.A. Gomez, and W.H. Akeson, (1981). "The time and history-dependent viscoelasticity properties of the canine medial collateral ligament." *Journal of Biomechanical Engineering* 103: 293-298.

[13] Yamamoto S., Kajzer, J., and E. Tanaka, (2000). "Development of high-speed tensile test system for ligaments and skeletal muscles", In *Human Biomechanics and Injury Prevention*, Ed. Kajzer J., Tanaka E., Yamada H., Springer: 167 – 172.

[14] Fung YC. (1967). "Elasticity of soft tissues in simple elongation." *Am J Physiol*; 213: 1532–1544.

[15] Weiss, J.A. (1994). "A constitutive model and finite element representation for transversely isotropic soft tissues." Ph.D. Dissertation, Department of Bioengineering, University of Utah; 1994.

[16] Stander, N., Eggleston T., Craig K., and W. Roux (2003), "LS-OPT User's Manual", Livermore Software Technology Corporation.

[17] Puso, M.A.. and Weiss J.A., 1998, "Finite Element Implementation of Anisotropic Quasi-Linear

Viscoelasticity Using a Discrete Spectrum Approximation," *J. Biomech. Eng.* 120: 62-70.

[18] Dhaliwal, T.S.; Beillas, P.; Chou, C.C.; Prasad, P.; Yang, K.H., and King, A.I., 2002, "Structural Response of Lower Leg Muscles in Compression: A Low Impact Energy Study Employing Volunteers, Cadavers and the Hybrid III" *Stapp Car Crash Journal* 46: 229-243.